Adsorption (2014) 20:251–259
DOI 10.1007/s10450-013-9568-6

Unusual chain length dependent adsorption of linear and branched alkanes on UiO-66

Tim Duerinck · Joeri F. M. Denayer

Received: 19 May 2013 / Accepted: 10 August 2013 / Published online: 29 August 2013
© Springer Science+Business Media New York 2013

Abstract In this work, the zero coverage adsorption properties of C_5–C_{10} *n*- and iso-alkanes on the UiO-66, UiO-66-Me and UiO-66-NO_2 metal–organic frameworks are studied by gas phase pulse chromatography. Analysis of enthalpy values, entropy values, Gibbs free energies and Henry constants reveals unusual chain length dependent adsorption behaviour of linear and branched alkanes, caused by the complex structure of the zirconium metal–organic framework UiO-66. The UiO-66 structure consists of a small, tetrahedral and large, octahedral cage. It is shown that at specific carbon chain lengths (e.g. C_6–C_7 for *n*-alkanes), distinctive jumps in adsorption enthalpy, entropy values and Henry constants occur. This chain length dependent effect is even more pronounced for 2- and 3-methyl alkanes and double branched alkanes. This distinctive shift in adsorption behaviour occurs at a molecular size that coincides with the cavity dimensions of the smallest, tetrahedral cage. The resulting selective adsorption arises from confinement effects and is function of both the molecular shape and size.

Keywords UiO-66 · Confinement · Adsorption · Alkanes

Electronic supplementary material The online version of this article (doi:10.1007/s10450-013-9568-6) contains supplementary material, which is available to authorized users.

T. Duerinck · J. F. M. Denayer (✉)
Department of Chemical Engineering, Vrije Universiteit Brussel, Pleinlaan 2, 1050 Brussel, Belgium
e-mail: joeri.denayer@vub.ac.be

1 Introduction

The metal organic framework UiO-66 was originally reported by Cavka et al. in their work on the synthesis of the isostructural Zr-MOF series UiO-66, UiO-67 and UiO-68 materials based on the inorganic brick $Zr_6O_4(OH)_4$ and 1,4-benzene-dicarboxylate (BDC) as organic linker for UiO-66 (Cavka et al. 2008). The complex structure consists of small tetrahedral (~7.5 Å) and large octahedral (~11 Å) cages. The given pore dimensions are approximations by fitting a sphere inside the pore. The complex structure was elucidated by a combination of XRD, NMR, vibration spectroscopy and computational optimizations (Valenzano et al. 2011). The average number of BDC-X linkers coordinated to a $Zr_6O_4(OH)_4$ cluster is 8–10 and not the theoretical achievable 12. The result of this incomplete coordination is the presence of defects or "holes" in the framework (Vermoortele et al. 2012). At elevated temperatures and high vacuum condition, a reversible dehydroxylation of the metal cluster occurs. This induces small conformational changes in the metal-oxo cluster and subsequently repositions the organic linkers (Valenzano et al. 2011; Devautour-Vinot et al. 2012). The change in structure does not compromise the structural integrity or stability of the framework. The effective size of the microporous windows appears to be temperature dependent due to the rotational motion of the benzene rings (Kolokolov et al. 2012). Furthermore the UiO-66 framework shows remarkable thermal, chemical and mechanical stability (Cavka et al. 2008; Schoenecker et al. 2012; Valenzano et al. 2011).

Isoreticular synthesis and incorporation of modified BDC linkers in the framework was reported for a variety of functionalities including amides, amino, nitro, halogen, alkyl, sulphonic. The most straightforward route is by use

of modified BDC linkers in the UiO-66 synthesis. An alternative route is post-synthetic modification. The latter often starts from the amino-UiO-66 and leads to amide or anhydride functionalities (Garibay and Cohen 2010; Foo et al. 2012; Kim et al. 2012a; b; Abid et al. 2012a; Morris et al. 2011; Zlotea et al. 2011; Kandiah et al. 2010). The crystal and particle size of the UiO-66 material can be controlled by modulated synthesis by introducing benzoic acid as a growth controlling agent (Schaate et al. 2011). The polarity of the structure is changed to a certain extend by employing modified linkers. This is illustrated by the reduced water adsorption on UiO-66-Me (Schoenecker et al. 2012), increased CO_2 uptake in the presence of sulphonic acid groups (Foo et al. 2012) or changing selectivity in catalysis (Vermoortele et al. 2012, 2011).

The UiO-66 framework was evaluated for gas based adsorptive applications (H_2, CH_4, CO_2) by several groups (Yang et al. 2012; Abid et al. 2012b; Chavan et al. 2012; Wiersum et al. 2011; Yang et al. 2011a, c; Zlotea et al. 2011; Soubeyrand-Lenoir et al. 2012, Nik et al. 2012). In humid conditions, CO_2 uptake remains unchanged (Soubeyrand-Lenoir et al. 2012). Incorporation of UiO-66-NH_2 in polymer membranes increased the CO_2 permeability in CO_2/CH_4 separations (Nik et al. 2012). Enhanced affinity of the dimethyl functionalized UiO-66 for CO_2 was reported (Huang et al. 2012). Reversed shape selectivity of hexane isomers and selective xylene adsorption in vapour and liquid phase has been reported (Barcia et al. 2011; Moreira et al. 2012; Mendes et al. 2013). The potential of the UiO-66 framework for these separations was evaluated experimentally and computationally in packed columns (Barcia et al. 2011; Moreira et al. 2012). A follow-up study using capillary GC confirmed and extended the work to alkylbenzenes (Chang and Yan 2012). In recent work, we have studied the adsorption of *n*-alkanes and cyclo-alkanes on UiO-66, and demonstrated the separation of cis- and trans-isomers of disubstituted cyclic stereoisomers (Duerinck et al. 2013). It was shown by experimental work and Monte Carlo simulations that shape and size effects play a determining role in the preferential adsorption of isomers at specific positions (large or small cage).

In this work, we focus on the adsorption of linear and branched alkanes by different techniques, using the concept of confinement factors. The trends in adsorption enthalpy, entropy and Gibbs free energy are rigorously analyzed and connected to confinement effect resulting from the interplay between molecular size, shape and the metal–organic framework topology.

2 Adsorption data and analysis

The inverse pulse chromatographic data of UiO-66 and functionalized variants (UiO-66-Me, UiO-66-NO_2) is reproduced from the recently published work (Duerinck et al. 2013). UiO-66 and functionalized variants (UiO-66-Me, UiO-66-NO_2) were synthesized according to published methods (Vermoortele et al. 2012). The different UiO-66-X materials were synthesized from an equimolar solution (1.5 mM) of $ZrCl_4$, the (functionalized) terephthalic acid and H_2O in DMF. The solution was poured in a Schott bottle and placed in an oven at 393 K for 10–24 h. After the synthesis, the metal–organic frameworks (MOF) was recovered by centrifugation. Structure was verified by XRD (Figure S1.). Adsorption equilibrium Henry constants were calculated from the first moment of the chromatographic response curves in the range of 473–573 K for UiO-66, 473–573 K for UiO-66-Me and 473–553 K for UiO-66-NO_2. From the temperature dependency of the Henry adsorption constants K′, the adsorption enthalpy ΔH_0 (kJ/mol) can be derived. A detailed explanation of the experimental setup and procedure was previously reported (Ocakoglu et al. 2002).

From an extensive data set of 70–80 molecules on the UiO-66 materials (native, UiO-66-Me, UiO-66-NO_2, UiO-66-Me_2), the subset of linear (as reference), single and double branched alkanes was taken. The adsorption properties of the branched alkanes subset is given in Table S1 but has received no detailed analysis so far. The Gibbs free energy values ΔG_0 (kJ/mol) were directly calculated from the Henry constants that were determined using published methods (Denayer et al. 1998b; Tielens et al. 2003). Given the knowledge of both ΔG_0 and ΔH_0, the entropy factor ΔS_0 is deducible:

$$\Delta G_0 = -RT \ln[K' \rho_c RT]$$

$$\Delta S_0 = -[\Delta G_0 - \Delta H_0]/T$$

with R ideal gas constant (J/[mol.K]), T Temperature (523 K), K′ Henry constant (at 523 K), ρ_c crystal density (kg/m^3).

In this work, the influence of carbon chain length on the adsorption properties of UiO-66 is investigated. In the further analysis of Henry constants, adsorption selectivity is calculated as the ratio of them for two components at a given reference temperature, 523 K in this case. The ratio is rounded down to 1 significant digit in all cases, although standard errors are 1–3 % in all cases.

$$\alpha_{K'} = \frac{K_i'}{K_j'}$$

with K_i' = Henry constant of adsorbate i, $\alpha_{K'}$ = adsorption selectivity at zero coverage, 523 K.

The confinement factor Z, developed for zeolitic systems and calculable from thermodynamic data obtained in inverse pulse chromatography, correlates well with the pore size for zeolites (Denayer and Baron 2005; Devriese

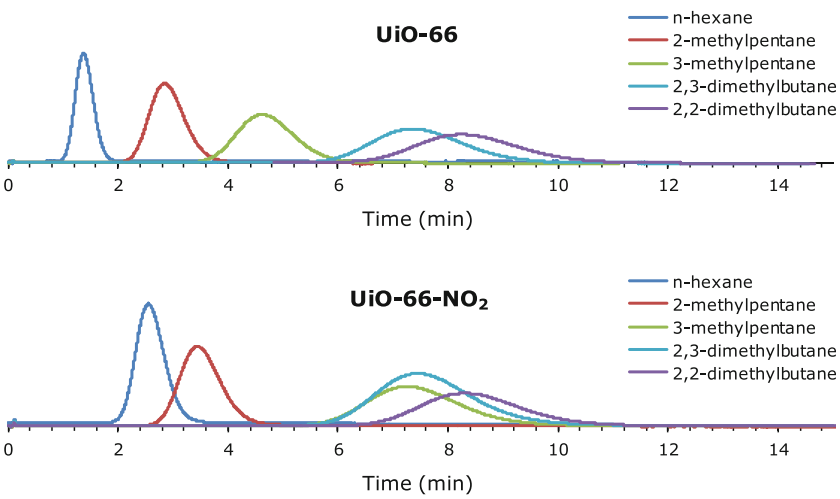

Fig. 1 Chromatographic profiles of linear and branched C6 isomers on UiO-66 and UiO-66-NO_2 at 523 K

et al. 2007). It quantifies the steric constrains imposed by a pore or cavity on the adsorbed molecule. Thus it can serve as a measure for the effective pore size that the adsorbate experiences.

$$Z = \frac{\gamma}{\alpha}$$

.

The values for α and γ are normally obtained from the linear regression of adsorption enthalpy ΔH_0 and entropy ΔS_0 factors as a function of the carbon number for *n*-alkanes. The factors δ and β are intercept values. In this work, these values are calculated between alkanes of N_c and N_{c+1} to allow for stepwise assessment as no general linear trend was obtained (see below).

$$-\Delta S_0 = \gamma N_C + \delta$$

$$-\Delta H_0 = \alpha N_C + \beta$$

The given geometrical discussion (below) is based on the size of "*ball-stick*" models and van der Waals volumes for guest molecules. *n*-Alkanes are approximated by the cylinders to take into account rotational mobility along their length axis. These values are computed from optimized geometrical structures in Materials Studio 5.0. The size and volume of the nanocages are determined computing the volume of a tetrahedron (small cage) or octahedron (large cage). The appropriate distances are measured between corner atoms, correcting for the van der Waals volume of the atoms.

3 Results and discussion

3.1 Chromatographic elution profiles

The metal–organic framework UiO-66 is able to discriminate between linear and branched alkanes, as illustrated in the chromatograms for C_6 isomers on UiO-66 and UiO-66-NO_2 in Fig. 1. Remarkably, the chromatographic profiles show a strong preference for single and double branched alkanes. This preference is called "inverse shape selectivity". UiO-66 materials strongly retain C_7 isomers: 2,3-dimethylpentane is retained 4.2 times longer than *n*-heptane on UiO-66, 4.0 times longer on UiO-66-Me and 2.9 times longer on UiO-66-NO_2 at 523 K. Very high selectivity factors of 6.6 and 6.9 were observed for 3,3-dimethylpentane over *n*-heptane on UiO-66 and UiO-66-Me. Most nanoporous materials preferentially

Table 1 Adsorption selectivity of branched over linear alkanes at 523 K

Molecule	UiO-66	UiO-66-Me	UiO-66-NO_2
2-Methylbutane	2.1	1.0	1.5
2-Methylpentane	1.8	1.4	1.4
3-Methylpentane	2.9	2.4	2.9
2,2-Dimethylbutane	5.3	3.8	3.3
2,3-Dimethylbutane	4.7	3.9	3.0
2-Methylhexane	1.2	1.1	1.3
3-Methylhexane	2.1	1.6	1.7
2,3-Dimethylpentane	4.2	4.0	2.9
2,4-Dimethylpentane	1.9	1.5	1.5
3,3-Dimethylpentane	6.6	6.9	4.2
2-Methylheptane	0.9	0.9	1.5
3-Methylheptane	1.1	1.0	1.5
4-Methylheptane	1.2	1.0	1.5
2,2-Dimethylhexane	1.3	1.1	1.4
2,4-Dimethylhexane	1.5	1.1	1.5
2,5-Dimethylhexane	0.8	0.7	1.3
2,2,4-Trimethylpentane	2.2	1.5	1.4
2-Methyloctane	0.9	–	0.9
2,3-Dimethylheptane	1.0	0.9	0.8
2,2,4-Trimethylhexane	1.4	0.8	0.7
3-Methylnonane	0.4	0.8	0.8
4-Methylnonane	0.7	0.5	0.7

adsorb linear alkanes over branched or cyclic isomers. For example MIL-47 retains *n*-heptane respectively 1.6 and 1.4 longer than 3-methylhexane and 2,3-dimethylpentane (Finsy et al. 2009). ZSM-5 shows preferential adsorption by a factor of 2.1 of *n*-heptane over 3-methylhexane (Denayer et al. 1998b). A few materials that show an inverse shape effect are SAPO-5, CHA and MCM-22 (Denayer et al. 2006a, b 2008, 2005; Huang et al. 2009). Such materials typically have narrow pores or complex cage structures with small windows. Confinement effects play an important role here. For example 2,2-dimethylbutane and 2,3-dimethylbutane have a selectivity factor of 1.56 and 1.51 over *n*-hexane on SAPO-5. On UiO-66 *n*-hexane, 2-methylpentane, 3-methylpentane, 2,3-dimethylpentane and 2,2-dimethylpentane are eluting sequentially. Selectivity factors compared to *n*-hexane are respectively 1.8, 2.9, 4.7 and 5.3. This corresponds with a shift from a linear to a more ellipsoidal or globular molecular shape. The same trend is observed for UiO-66-Me and UiO-66-NO_2 but the relative differences in retention time and adsorption selectivity changes. This elution sequence is in accordance with the results of Barcia et al. at 473 K and Mendes et al. (Barcia et al. 2007; Mendes et al. 2013). However, the adsorption selectivity (Table 1) at zero coverage are higher than those reported at higher partial pressure. Selectivity factors of all measured branched over linear alkanes are given in Table 1.

It should be noted that the adsorption selectivity of branched over linear alkanes in general follows the same trends for the different UiO-66 forms: isomers with double methyl groups on the main carbon chain are retained much stronger for C_6 and C_7 isomers. The explicit preference vanishes for the C_8, C_9 and C_{10} isomers. In the case of C_9 and C_{10} isomers the linear and not branched alkanes are much stronger retained: 4-methylnonane has selectivity factors of 0.7 for UiO-66, 0.5 for UiO-66-Me and 0.7 for UiO-66-NO_2. When comparing the different UiO-66 forms, the native UiO-66 in general has higher selectivity

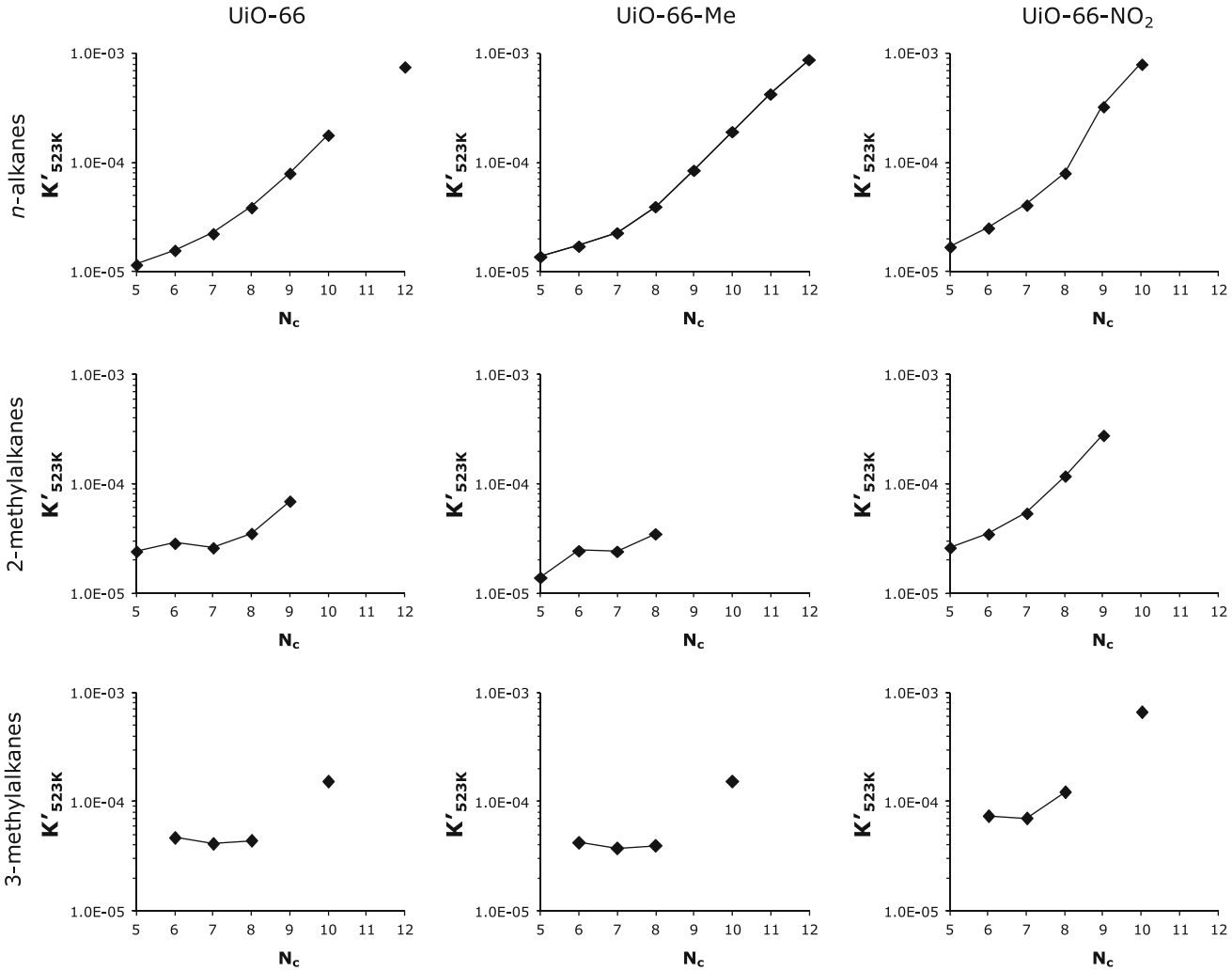

Fig. 2 Henry constants ($K'_{523\ K}$, mol/[kg.Pa]) of linear, 2-methyl alkanes and 3-methyl alkanes as a function of the carbon number (N_c) on UiO-66, UiO-66-Me and UiO-66-NO_2 at 523 K

factors for C_5–C_7 alkanes: e.g. 2,3-dimethylbutane/hexane is respectively 4.7, 3.9 and 3.0 for UiO-66, UiO-66-Me and UiO-66-NO_2. An exception is 3,3-dimethylpentane on UiO-66-Me: separation factor of 6.9 compared to 6.6 for UiO-66 and 4.2 for UiO-66-NO_2. The cages of UiO-66-NO_2 allow for better separation of C_8 isomers. The authors conclude from this that selectivity factors vary depending on the adsorbate-adsorbent combination and are size (shape and length) dependent.

3.2 Chain length dependency of adsorption properties

The size dependent adsorption behavior is clearly visible in Figs. 2, 3. Here the evolution of Henry constants, Gibbs free energy, adsorption enthalpy and entropy is plotted as a function of the total carbon number for *n*-alkanes, 2-methyl and 3-methylalkanes. On most microporous solids exhibiting a pore system consisting of channels, a perfect exponential trend for Henry constants is observed for *n*-alkanes and isostructural branched alkanes (Duerinck et al. 2012a, b; Devriese et al. 2007; Finsy et al. 2009; Denayer and Baron 1997; Denayer et al. 1998a, b). On this material, with a structure containing small and large cages, a non-linear trend is observed, even for linear alkane chains curved or sigmoidal trends, even local minima are found. When Henry constants are plotted in a logarithmic scale (Fig. 2), large deviations from linearity are observed. The Henry constants $K'_{523\ K}$ only increase by 8 % between 2-methylpentane and 2-methylheptane on UiO-66 whereas this is a 170 % between 2-methylpentane and 2-methylnonane. Similarly, only a limited change (~6 %) in Henry constants $K'_{523\ K}$ is observed for 3-methylalkanes between C_6 and C_8.

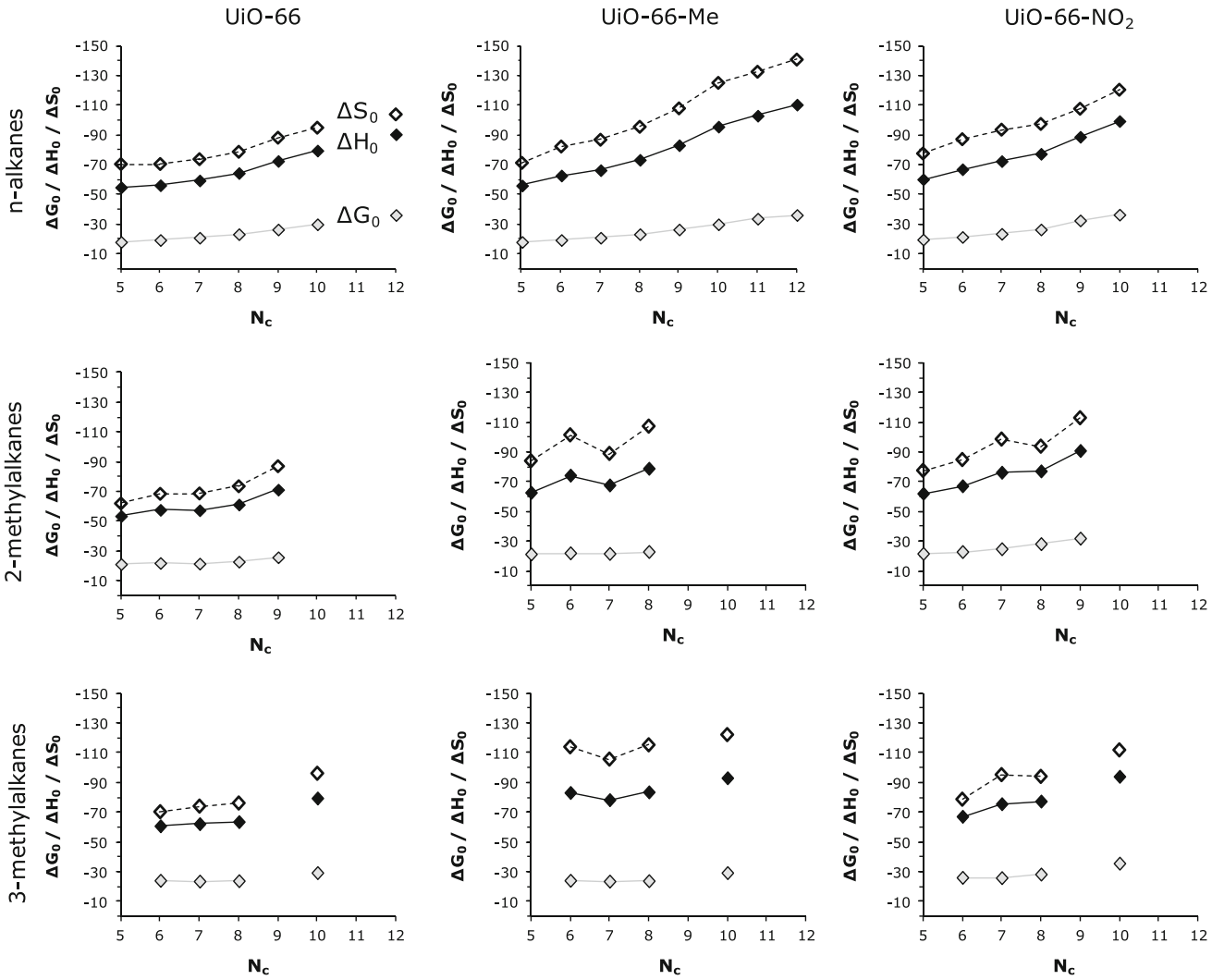

Fig. 3 Gibbs free energy (ΔG_0, kJ/mol—*empty symbols*), adsorption enthalpy (ΔH_0, kJ/mol—full, *black symbols*) and entropy (ΔS_0, J/[mol.K]—full, *grey symbols*) of linear, 2-methyl alkanes and 3-methyl alkanes as a function of the carbon number (N_c) on UiO-66, UiO-66-Me and UiO-66-NO_2

A distinctive drop in Henry constants is observed for 2-methyl and 3-methylalkanes between C_6 and C_7 (Fig. 2). From C_8 on, the Henry constants increase again. This drop is observed for the native and functionalized UiO-66 materials. The Gibbs free energy (Fig. 3) shows smoother evolution with the carbon number but the jumps in properties are clearly visible for enthalpy and entropy values. Normally, adsorption enthalpy and entropy vary linearly with chain length. An increase of adsorption enthalpy by 6–6.5 kJ/mol per added carbon number was previously reported for Y zeolites, 10–12 kJ/mol Beta, Mordenite, ZSM-5 and ZSM-22 (Denayer et al. 1998b). Here a decrease (absolute values) in adsorption properties values is observed for certain guest host combination: e.g. 2-methylpentane and 2-methylhexane (4–7 units) or 3-methylpentane and 3-methylhexane (5–8 units) on UiO-66-Me. The average trend in adsorption enthalpy (from linear regression) is 4.4 kJ/mol for UiO-66, 5.5 kJ/mol for UiO-66-Me and 6.4 kJ/mol for UiO-66-NO_2 per added carbon atom. Compared to Na-Y and Na-USY, the adsorption strength is 5–10 kJ/mol higher (more negative enthalpy value), which is explained by the smaller size of the tetrahedral cages of UiO-66.

The jumps in adsorption properties coincide with the size at which a molecule is no longer able to fit easily inside the smallest, tetrahedral pore (largest dimension molecule >largest dimension tetrahedral cage $\sim$11 Å) but has to adopt a folded state. *n*-Pentane fills about 80 % ($\sim$144 Å^3) of the pore volume of the smallest pore ($\sim$175 Å^3), *n*-hexane nearly completely ($\sim$172 Å^3). Thus, longer carbon chains have to be folded densely or have one or more groups in the window region. As the octahedral cage is about three times as large ($\sim$512 Å^3), no confinement effects are expected there. It was previously shown by molecular simulations for *n*-alkanes that an *n*-alkane chain with 6 carbon atoms still fits inside the tetrahedral cage but longer chains only fit in a densely folded conformation (Duerinck et al. 2013). Longer carbon chains (C_8–C_{10}) are statistically distributed between the tetrahedral and octahedral cages, with a dense population of long chains in the latter one.

The experimental data suggests interplay between molecular shape, size and the metal–organic framework cavities. The confinement factor offers an estimate of how well a molecule fits in a cage. This parameter was introduced for zeolitic structures but can be applied to metal–organic frameworks as well (Denayer and Baron 2005). In this work, the match between adsorbent and adsorbate is estimated by observing changes in confinement factor between isostructural molecules with n and $n + 1$ carbon atoms. Results are given in Table 2. A decrease in confinement factor indicates that the average distance between adsorbate and the pore wall increases. Within the subset of *n*-alkanes, UiO-66-Me has the highest confinement factors. On average the confinement effects are much more pronounced for the functionalized UiO-66 materials. The conclusion that can be drawn from this observation is that the methyl or nitro group reduces the effective pore size. The inner pore volume of the tetrahedral cage is approximately 175 Å^3 for the native UiO-66 material. The linkers are essentially randomly orientated in the framework structure. From a statistical point a view two or three functional groups ($-CH_3$ or NO_2) will be on average orientated inside a cage. The van der Waals volume of the methyl and nitro group corresponds to respectively 24.3 and 24.6 Å^3. When a single functional group is completely orientated inside the pore, an effective pore volume reduction of ca. 13 % is expected. This effective pore reduction can also be deducted from the average confinement factor for C_4–C_{12} *n*-alkanes series: 0.98 for UiO-66, 1.27 for UiO-66-Me and 1.05 for UiO-66-NO_2. No specific interaction with the nitro group was observed for the studied alkane series. This observation is in line with the work Yang et al. (2011a, b). They reported that the chemical environment inside the framework's cages is influenced by the chemical nature of the functional group on the BDC linker but no specific interaction sites were

Table 2 Confinement factor Z of C_5–C_{12} linear and branched alkanes on UiO-66, UiO-66-Me and UiO-66-NO_2

Confinement factor from *n*-C_x to *n*-C_{x+1}	UiO-66	UiO-66-Me	UiO-66-NO_2
n-Pentane to *n*-hexane	0.05	1.64	1.42
n-Hexane to *n*-heptane	1.01	1.26	1.18
n-Heptane to *n*-octane	1.00	1.25	0.78
n-Octane to *n*-nonane	1.17	1.26	0.89
n-Nonane to *n*-decane	0.96	1.37	1.21
n-Decane to *n*-undecane	–	1.01	–
n-Undecane to *n*-dodecane	–	1.10	–
2-Methylbutane to 2-methylpentane	1.57	1.51	1.44
2-Methylpentane to 2-methylhexane	−0.89	1.89	1.51
2-Methylhexane to 2-methylheptane	1.26	1.64	−5.27
2-Methylheptane to 2-methyloctane	1.35	–	1.39
3-Methylpentane to 3-methylhexane	2.64	1.71	1.96
3-Methylhexane to 3-methylheptane	1.52	1.82	−0.68
2,3-Dimethylbutane to 2,4-dimethylpentane	0.92	0.98	1.11
2,4-Dimethylpentane to 2,5-dimethylhexane	0.98	1.58	1.36

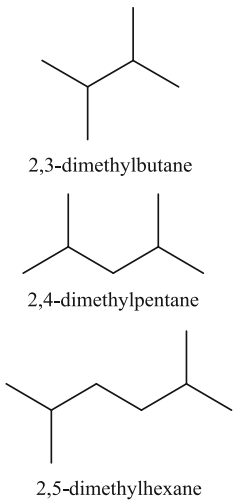

Fig. 4 Molecular structure of 2,3-dimethylbutane, 2,4-dimethylpentane and 2,5-dimethylhexane

found for CH_4 on the UiO-66 materials. However they showed that in simulations that specific interactions between CO_2 and polar functionalities (e.g. nitro group in UiO-66-NO_2) are likely to occur.

A local minimum is observed between *n*-heptane and *n*-octane. This confirms a switch in preferential adsorption site from the tetrahedral to the octahedral cage. Drastic drops in confinement factors are observed between 2-methylpentane and 2-methylhexane ($Z = -0.89$) on UiO-66, 2-methylhexane and 2-methylheptane ($Z = -5.27$) on UiO-66-NO_2 and 3-methylhexane and 3-methylheptane ($Z = -0.68$) on UiO-66-NO_2. The negative factors results from a negative slope in adsorption enthalpy or entropy between N_c and N_{c+1} (not both).

The subtle interplay of molecular and framework size and shape is nicely expressed when considering the subset of 2,3-dimethylbutane, 2,4-dimethylpentane and 2,5-dimethylhexane (Fig. 4). These isomers have an iso branching structure at both sides of the main carbon chain which is elongated from C_4 to C_6. When considering this series of molecules, a decreasing trend in adsorption properties is observed for all adsorption parameters on the native UiO-66 material (Fig. 5). The adsorption enthalpy stepwise decreases from −66.6 to −61.7 kJ/mol and then −59.7 kJ/mol. Analogue, adsorption entropy goes from −77.4 to −72.9 J/[mol.K] and −70.9 J/[mol.K]. The Gibbs free energy values and evolution thereof for UiO-66-Me and UiO-66-NO_2 are similar to those for the native UiO-66 material. A pronounced downward slope of adsorption enthalpy and entropy values is observed for UiO-66-Me. Entropy factors play a much bigger effect due to effective pore size reduction on the functionalized materials: −15 J/[mol.K] between 2,3-dimethylbutane and 2,5-dimethylhexane on UiO-66-Me. For UiO-66-NO_2 a downward step is observed between 2,3-dimethylbutane and 2,4-dimethylpentane (−2 units) but an upward step in noted between 2,4-dimethylpentane and 2,5-dimetylhexane (+8 to 10 units). The adsorption selectivity $\alpha_{K'}$ shows that 2,3-dimethylbutane (N_{c-2}) and 2,4-dimethylpentane (N_{c-1}) are respectively 2.25 and 1.26 times more retained

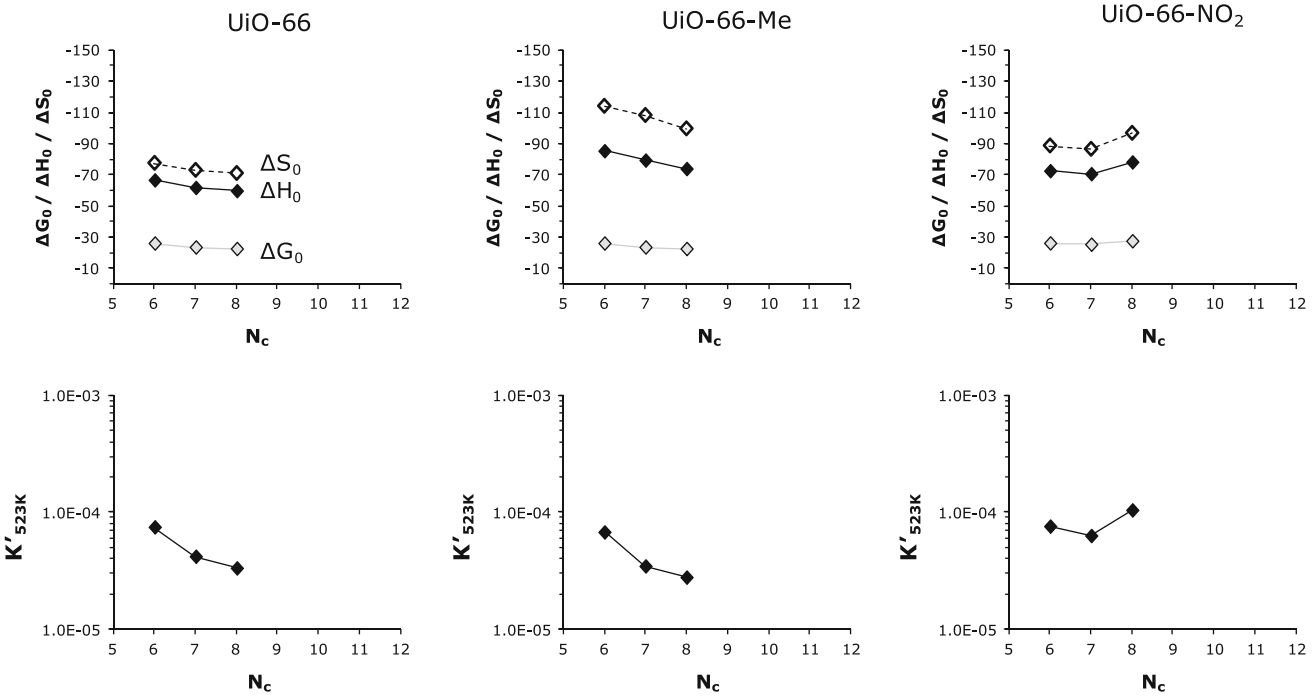

Fig. 5 Gibbs free energy (ΔG_0, kJ/mol), adsorption enthalpy (ΔH_0, kJ/mol), adsorption entropy (ΔS_0, J/[mol.K]) and Henry constants ($K'_{523\ K}$, mol/[kg.Pa]) as a function of carbon number for 2,3-dimethylbutane, 2,4-dimethylpentane and 2,5-dimethylhexane

than 2,5-dimethylhexane (N_c) on UiO-66. The same trend is observed for UiO-66-Me: $\alpha_{K'} = 2.44$ for 2,3-dimethylbutane and $\alpha_{K'} = 1.25$ for 2,4-dimethylpentane (N_{c-1}).

4 Conclusion

It was unambiguously shown that there is a chain length dependent effect in the adsorption of saturated alkanes in UiO-66 structures. The data shows that this effect coincides with the moment that a carbon chain no longer easily fits inside the tetrahedral cage without significant folding. The influence of entropy values underlines the interplay between adsorbate–adsorbent size and shape. Confinement effect plays an important role in observed chromatographic retention times. Remarkably, this results in a lower retention of some hydrocarbons of higher carbon number as compared to their N_{c-1} or N_{c-2} counterparts.

Acknowledgments The authors wish to thank Prof. Dr. Dirk E. De Vos and co-workers for providing the UiO-66 materials.

References

Abid, H.R., Ang, H.M., Wang, S.: Effects of ammonium hydroxide on the structure and gas adsorption of nanosized Zr-MOFs (UiO-66). Nanoscale **4**(10), 3089–3094 (2012a)

Abid, H.R., Tian, H., Ang, H.M., Tade, M.O., Buckley, C.E., Wang, S.: Nanosize Zr-metal organic framework (UiO-66) for hydrogen and carbon dioxide storage. Chem Eng J **187**, 415–420 (2012b)

Barcia, P.S., Guimaraes, D., Mendes, P.A., Silva, J.A., Guillerm, V., Chevreau, H., Serre, C., Rodrigues, A.E.: Reverse shape selectivity in the adsorption of hexane and xylene isomers in MOF UiO-66. Microporous Mesoporous Mater **139**(1–3), 67–73 (2011)

Barcia, P.S., Zapata, F., Silva, J.A.C., Rodrigues, A.E., Chen, B.: Kinetic separation of hexane isomers by fixed-bed adsorption with a microporous metal–organic framework. J Phys Chem B **111**(22), 6101–6103 (2007). doi:10.1021/jp0721898

Cavka, J.H., Jakobsen, S., Olsbye, U., Guillou, N., Lamberti, C., Bordiga, S., Lillerud, K.P.: A new zirconium inorganic building brick forming metal organic frameworks with exceptional stability. J Am Chem Soc **130**(42), 13850–13851 (2008). doi:10.1021/ja8057953

Chang, N., Yan, X.P.: Exploring reverse shape selectivity and molecular sieving effect of metal–organic framework UIO-66 coated capillary column for gas chromatographic separation. J Chromatogr A **1257**, 116–124 (2012)

Chavan, S., Vitillo, J.G., Gianolio, D., Zavorotynska, O., Civalleri, B., Jakobsen, S., Nilsen, M.H., Valenzano, L., Lamberti, C., Lillerud, K.P., Bordiga, S.: H-2 storage in isostructural UiO-67 and UiO-66 MOFs. Phys Chem Chem Phys **14**(5), 1614–1626 (2012)

Denayer, J.F., Baron, G.V., Martens, J.A., Jacobs, P.A.: Chromatographic study of adsorption of *n*-alkanes on zeolites at high temperatures. J Phys Chem B **102**(17), 3077–3081 (1998a). doi:10.1021/jp972328t

Denayer, J.F., Souverijns, W., Jacobs, P.A., Martens, J.A., Baron, G.V.: High-temperature low-pressure adsorption of branched C-5-C-8 alkanes on zeolite beta, ZSM-5, ZSM-22, zeolite Y, and mordenite. J Phys Chem B **102**(23), 4588–4597 (1998b)

Denayer, J.F.A., Devriese, L.I., Couck, S., Martens, J., Singh, R., Webley, P.A., Baron, G.V.: Cage and Window Effects in the Adsorption of *n*-Alkanes on Chabazite and SAPO-34. J Phys Chem C **112**(42), 16593–16599 (2008). doi:10.1021/jp804349v

Denayer, J.F.M., Baron, G.V.: Adsorption of normal and branched paraffins in faujasite zeolites NaY, HY, Pt/NaY and USY. Adsorpt-J Int Adsorpt Soc **3**(4), 251–265 (1997). doi:10.1007/bf01653628

Denayer, J.F.M., Baron, G.V.: The confinement factor: A thermodynamic parameter to characterize microporous adsorbents. Adsorpt-J Int Adsorpt Soc **11**, 85–90 (2005)

Denayer, J.F.M., Daems, I., Baron, G.V.: Adsorption and reaction in confined spaces. Oil & Gas Sci Technol **61**(4), 561–569 (2006a)

Denayer, J.F.M., Ocakoglu, R.A., Arik, I.C., Kirschhock, C.E.A., Martens, J.A., Baron, G.V.: Rotational entropy driven separation of alkane/isoalkane mixtures in zeolite cages. Angew Chem-Int Ed **44**(3), 400–403 (2005). doi:10.1002/anie.200454058

Denayer, J.F.M., Ocakoglu, R.A., Thybaut, J., Marin, G., Jacobs, P., Martens, J., Baron, G.V.: *n*- and isoalkane adsorption mechanisms on zeolite MCM-22. J Phys Chem B **110**(17), 8551–8558 (2006b). doi:10.1021/jp060657s

Devautour-Vinot, S., Maurin, G., Serre, C., Horcajada, P., da Cunha, D.P., Guillerm, V., Costa, EdS, Taulelle, F., Martineau, C.: Structure and dynamics of the functionalized MOF type UiO-66(Zr): NMR and dielectric relaxation spectroscopies coupled with DFT calculations. Chem Mater **24**(11), 2168–2177 (2012)

Devriese, L.I., Cools, L., Aerts, A., Martens, J.A., Baron, G.V., Denayer, J.F.M.: Shape selectivity in adsorption of *n*- and isoalkanes on a zeotile-2 microporous/mesoporous hybrid and mesoporous MCM-48. Adv Funct Mater **17**(18), 3911–3917 (2007)

Duerinck, T., Bueno-Perez, R., Vermoortele, F., De Vos, D.E., Calero, S., Baron, G.V., Denayer, J.F.M.: Understanding hydrocarbon adsorption in the UiO-66 metal–organic framework: separation of (Un)saturated linear, branched, cyclic adsorbates, including stereoisomers. J Phys Chem C **117**(24), 12567–12578 (2013). doi:10.1021/jp402294h

Duerinck, T., Couck, S., Vermoortele, F., De Vos, D.E., Baron, G.V., Denayer, J.F.M.: Pulse gas chromatographic study of adsorption of substituted aromatics and heterocyclic molecules on MIL-47 at zero coverage. Langmuir **28**(39), 13883–13891 (2012a). doi:10.1021/la3027732

Duerinck, T., Leflaive, P., Arik, I.C., Pirngruber, G., Meynen, V., Cool, P., Martens, J.A., Baron, G.V., Faraj, A., Denayer, J.F.M.: Experimental and statistical modeling study of low coverage gas adsorption of light alkanes on meso-microporous silica. Chem Eng J **179**, 52–62 (2012b). doi:10.1016/j.cej.2011.10.032

Finsy, V., Calero, S., Garcia-Perez, E., Merkling, P.J., Vedts, G., De Vos, D.E., Baron, G.V., Denayer, J.F.M.: Low-coverage adsorption properties of the metal–organic framework MIL-47 studied by pulse chromatography and Monte Carlo simulations. Phys Chem Chem Phys **11**(18), 3515–3521 (2009). doi:10.1039/b822247a

Foo, M.L., Horike, S., Fukushima, T., Hijikata, Y., Kubota, Y., Takata, M., Kitagawa, S.: Ligand-based solid solution approach to stabilisation of sulphonic acid groups in porous coordination polymer $Zr_6O_4(OH)(4)(BDC)(6)$ (UiO-66). Dalton Trans **41**(45), 13791–13794 (2012). doi:10.1039/c2dt31195j

Garibay, S.J., Cohen, S.M.: Isoreticular synthesis and modification of frameworks with the UiO-66 topology. Chem Commun **46**(41), 7700–7702 (2010)

Huang, S., Finsy, V., Persoons, J., Telling, M.T.F., Baron, G.V., Denayer, J.F.M.: Rotation dynamics of 2-methyl butane and n-pentane in MCM-22 zeolite: a molecular dynamics simulation

study. Phys Chem Chem Phys **11**(16), 2869–2875 (2009). doi:10.1039/b819334g

Huang, Y., Qin, W., Li, Z., Li, Y.: Enhanced stability and CO2 affinity of a UiO-66 type metal–organic framework decorated with dimethyl groups. Dalton Trans **41**(31), 9283–9285 (2012)

Kandiah, M., Nilsen, M.H., Usseglio, S., Jakobsen, S., Olsbye, U., Tilset, M., Larabi, C., Quadrelli, E.A., Bonino, F., Lillerud, K.P.: Synthesis and stability of tagged UiO-66 Zr-MOFs. Chem Mater **22**(24), 6632–6640 (2010)

Kim, M., Cahill, J.F., Fei, H., Prather, K.A., Cohen, S.M.: Postsynthetic ligand and cation exchange in robust metal–organic frameworks. J Am Chem Soc **134**(43), 18082–18088 (2012a). doi:10.1021/ja3079219

Kim, M., Cahill, J.F., Su, Y., Prather, K.A., Cohen, S.M.: Postsynthetic ligand exchange as a route to functionalization of 'inert' metal–organic frameworks. Chem Sci **3**(1), 126–130 (2012b)

Kolokolov, D.I., Stepanov, A., Guillerm, V., Serre, C., Frick, B., Jobic, H.: Probing the dynamics of the porous Zr terephthalate UiO-66 framework using H-2 NMR and neutron scattering. J Phys Chem C **116**(22), 12131–12136 (2012)

Mendes, P.A.P., Ragon, F., Rodrigues, A.E., Horcajada, P., Serre, C., Silva, J.A.C.: Hexane isomers sorption on a functionalized metal–organic framework. Microporous Mesoporous Mater **170**, 251–258 (2013). doi:10.1016/j.micromeso.2012.12.017

Moreira, M.A., Santos, J.C., Ferreira, A.F., Loureiro, J.M., Ragon, F., Horcajada, P., Shim, K.E., Hwang, Y.K., Lee, U., Chang, J.S., Serre, C., Rodrigues, A.E.: Reverse shape selectivity in the liquid-phase adsorption of xylene isomers in zirconium terephthalate MOF UiO-66. Langmuir **28**(13), 5715–5723 (2012)

Morris, W., Doonan, C.J., Yaghi, O.M.: Postsynthetic modification of a metal–organic framework for stabilization of a hemiaminal and ammonia uptake. Inorg Chem **50**(15), 6853–6855 (2011)

Nik, O.G., Chen, X.Y., Kaliaguine, S.: Functionalized metal organic framework-polyimide mixed matrix membranes for CO_2/CH_4 separation. J Membr Sci **413**, 48–61 (2012)

Ocakoglu, R.A., Denayer, J.F.M., Marin, G.B., Martens, J.A., Baron, G.V.: Tracer chromatographic study of pore and pore mouth adsorption of linear and monobranched alkanes on ZSM-22 zeolite. J Phys Chem B **107**(1), 398–406 (2002). doi:10.1021/jp0264533

Schaate, A., Roy, P., Godt, A., Lippke, J., Waltz, F., Wiebcke, M., Behrens, P.: Modulated synthesis of Zr-based metal–organic frameworks: from nano to single crystals. Chemistry **17**(24), 6643–6651 (2011)

Schoenecker, P.M., Carson, C.G., Jasuja, H., Flemming, C.J., Walton, K.S.: Effect of water adsorption on retention of structure and surface area of metal–organic frameworks. Ind Eng Chem Res **51**(18), 6513–6519 (2012)

Soubeyrand-Lenoir, E., Vagner, C., Yoon, J.W., Bazin, P., Ragon, F., Hwang, Y.K., Serre, C., Chang, J.S., Llewellyn, P.L.: How water fosters a remarkable 5-fold increase in low-pressure CO2 uptake within mesoporous MIL-100(Fe). J Am Chem Soc **134**(24), 10174–10181 (2012)

Tielens, F., Denayer, J.F.M., Daems, I., Baron, G.V., Mortier, W.J., Geerlings, P.: Adsorption of the butene isomers in faujasite: a combined ab-initio theoretical and experimental study. J Phys Chem B **107**(40), 11065–11071 (2003). doi:10.1021/jp0223760

Valenzano, L., Civalleri, B., Chavan, S., Bordiga, S., Nilsen, M.H., Jakobsen, S., Lillerud, K.P., Lamberti, C.: Disclosing the complex structure of UiO-66 Metal Organic Framework: a synergic combination of experiment and theory. Chem Mater **23**(7), 1700–1718 (2011)

Vermoortele, F., Ameloot, R., Vimont, A., Serre, C., De Vos, D.: An amino-modified Zr-terephthalate metal–organic framework as an acid-base catalyst for cross-aldol condensation. Chem Commun **47**(5), 1521–1523 (2011)

Vermoortele, F., Vandichel, M., Van de Voorde, B., Ameloot, R., Waroquier, M., Van Speybroeck, V., De Vos, D.E.: Electronic effects of linker substitution on Lewis acid catalysis with metal–organic frameworks. Angew Chem-Int Ed **51**(20), 4887–4890 (2012)

Wiersum, A.D., Soubeyrand-Lenoir, E., Yang, Q., Moulin, B., Guillerm, V., Ben Yahia, M., Bourrelly, S., Vimont, A., Miller, S., Vagner, C., Daturi, M., Clet, G., Serre, C., Maurin, G., Llewellyn, P.L.: An evaluation of UiO-66 for gas-based applications. Chemistry **6**(12), 3270–3280 (2011)

Yang, Q., Guillerm, V., Ragon, F., Wiersum, A.D., Llewellyn, P.L., Zhong, C., Devic, T., Serre, C., Maurin, G.: CH4 storage and CO2 capture in highly porous zirconium oxide based metal–organic frameworks. Chem Commun **48**(79), 9831–9833 (2012). doi:10.1039/c2cc34714h

Yang, Q., Jobic, H., Salles, F., Kolokolov, D., Guillerm, V., Serre, C., Maurin, G.: Probing the dynamics of CO_2 and CH_4 within the porous zirconium terephthalate UiO-66(Zr): a synergic combination of neutron scattering measurements and molecular simulations. Chem-An Eur J **17**(32), 8882–8889 (2011a)

Yang, Q., Wiersum, A.D., Jobic, H., Guillerm, V., Serre, C., Llewellyn, P.L., Maurin, G.: Understanding the thermodynamic and kinetic behavior of the CO_2/CH_4 gas mixture within the porous zirconium terephthalate UiO-66(Zr): a joint experimental and modeling approach. J Phys Chem C **115**(28), 13768–13774 (2011b)

Yang, Q., Wiersum, A.D., Llewellyn, P.L., Guillerm, V., Serred, C., Maurin, G.: Functionalizing porous zirconium terephthalate UiO-66(Zr) for natural gas upgrading: a computational exploration. Chem Commun **47**(34), 9603–9605 (2011c)

Zlotea, C., Phanon, D., Mazaj, M., Heurtaux, D., Guillerm, V., Serre, C., Horcajada, P., Devic, T., Magnier, E., Cuevas, F., Ferey, G., Llewellyn, P.L., Latroche, M.: Effect of NH_2 and CF_3 functionalization on the hydrogen sorption properties of MOFs. Dalton Trans **40**(18), 4879–4881 (2011)